NBO电荷计算对电中性原理的检验

徐嘉伟[1]　邓力克[1]　张浩哲[1]　张焕禹[1]　罗羽晨[1]
颜馨雅[1]　包建春[1]　方　敏[*,1,2,3]　吴　勇[*,1]

([1]南京师范大学化学与材料科学学院,江苏省生物功能材料协同创新中心,
江苏省新型动力电池重点实验室,南京　210023)
([2]南京师范大学,江苏省大规模复杂系统数值模拟重点实验室,南京　210023)
([3]南京大学,配位化学国家重点实验室,南京　210023)

摘要：我们在B3LYP/6-31++G(d,p)计算级别下计算了$[M(H_2O)_6]^{3+}$(M=Sc~Co)、$[Co(III)L_6]$(L=F^-、H_2O、NH_3、CN^-),以及基于α-Al_2O_3晶体结构搭建的铝氧簇$Al_3O(OH)_7(H_2O)_5$ (**Al₃**)和$Al_6O_6(OH)_6(H_2O)_5$ (**Al₆**)的NBO电荷。除$[Co(NH_3)_6]^{3+}$外,其它化合物均不符合经典教科书中的电中性原理,具有超出−1~+1范围的电荷。此外,我们发现中心原子的电荷受到配位原子种类的极大影响,而这一规律未在电中性原理的表述中。计算结果表明,从$[CoF_6]^{3-}$到$[Co(CN)_6]^{3-}$,中心离子上所带电荷量从+1.639变化至−1.360,且中心离子上所带电荷随其离子势的增大而降低。另外基于对铝氧簇的计算,我们预测α-Al_2O_3中的Al原子所带电荷应为2.1±0.1。

关键词：电中性原理；理论与计算化学；NBO电荷；密度泛函理论
中图分类号：O641.12　　　**文献标识码：**A　　　**文章编号：**1001-4861(2020)11-2157-12
DOI：10.11862/CJIC.2020.236

Verifying Principle of Electroneutrality by NBO Charge Calculations

XU Jia-Wei[1]　　DENG Li-Ke[1]　　ZHANG Hao-Zhe[1]　　ZHANG Huan-Yu[1]

LUO Yu-Chen[1]　　YAN Xin-Ya[1]　　Bao Jian-Chun[1]　　FANG Min[*,1,2,3]　　WU Yong[*,1]
([1]*Jiangsu Key Laboratory of New Power Batteries, Jiangsu Collaborative Innovation Center of Biomedical Functional*
Materials, School of Chemistry and Materials Science, Nanjing Normal University, Nanjing 210023, *China*)
([2]*Jiangsu Key Laboratory for Numerical Simulation of Large Scale Complex Systems* (*NSLSCS*),
Nanjing Normal University, Nanjing 210023, *China*)
([3]*State Key Laboratory of Coordination Chemistry, Nanjing University, Nanjing* 210023, *China*)

Abstract: NBO charges of $[M(H_2O)_6]^{3+}$ (M=Sc~Co), $[Co(III)L_6]$ (L=F^-, H_2O, NH_3, CN^-), $Al_3O(OH)_7(H_2O)_5$ (**Al₃**) and $Al_6O_6(OH)_6(H_2O)_5$ (**Al₆**) created based on α-Al_2O_3 were calculated at B3LYP/6-31++G(d,p) level of density functional theory (DFT). Except for $[Co(NH_3)_6]^{3+}$, they all violate the principle of electroneutrality (**EN**) by having charges outside the range of +1 to −1. In addition, the charge for the central metal ion is drastically influenced by the type of the coordination atoms, which is not included in the current **EN** principle. The charges of Co^{3+} in $[CoF_6]^{3-}$ and $[Co(CN)_6]^{3-}$ were found to be 1.639 and −1.360, respectively. When the ionic potential of the central atom increases, its charge would decrease. Based on our calculation, we predict the charge of Al in α-Al_2O_3 is 2.1±0.1.

Keywords: principle of electroneutrality; theoretical and computational chemistry; NBO charge; density functional theory

0 Introduction

It is well-known that free ions, such as Cu^{2+}, is unstable in aqueous solution, having a strong tendency to form hydrate ions[1-2]. In non-aqueous solvent, they will also coordinate with solvent molecules. This phenomenon is the result of electrostatic properties of molecules or ions, which respond to the environment through polarization by the local electric field[3]. Ions with smaller radii and higher charges have strong polarizing ability, while ions with larger radii will be easier to be polarized. Hard-soft acid and base (HSAB) theory rooted in these concepts[4-7].

To evaluate polarization capacities of ions[8-9], Cartledge coined the concept of ionic potential ($\varphi = Z/r$) where Z is the charge of an ion and r represents its radius. Later, Xu proposed to use Z^2/r to evaluate the polarization capacities of ions[10-13]. These parameters have advantages in quantitative calculations and explained experimental results commendably, having been accepted widely in high-level chemistry education and scientific studies nowadays. One consequence of polarization is that electrons are redistributed to reduce the electrostatic force between two entities when approaching to form a chemical bond. Thus, the polarization effect will reduce the charge of the ions and contribute to the covalent bonding of the bond. This is the reason why absolute ionic or covalent bonds between two different elements do not exist[14-16]. Only in some nonpolar covalent ones, bonding electrons are equally distributed between two atoms, and pure covalent bonds are formed. A chemical bond usually has some ionic character and some covalent character. The strength of a chemical bond is the results of both contributions.

Early in 1948, Pauling proposed the principle of electroneutrality (**EN**). "It has seemed to me likely that in general all of the atoms in the complexes that constitute stable chemical substances have resultant electrical charges smaller than those shown by these most electropositive and electronegative atoms in their compounds with one another, and I have accordingly formulated the postulate of the essential electrical neutrality of atoms: namely, that the electronic structure of substances is such as to cause each atom to have essentially zero resultant electrical charge, the amount of leeway being not greater than about ±1/2, and these resultant charges are possessed mainly by the most electropositive and electronegative atoms, and are distributed in such a way as to correspond to electrostatic ability"[17]. Huheey et al. wrote in the Inorganic Chemistry textbook, "Pauling suggested that complexes would be most stable when the electronegativity of the ligand was such that the metal achieved a condition of essentially zero net electrical charge. This tendency for zero or low electrical charges on atoms is a rule-of-thumb known as the electroneutrality principle, and it is used to make predictions regarding electronic structure in many types of compounds, not only complexes" [18]. Crabtree in his Organometallic Chemistry text book wrote about the **EN** principle, "Linus Pauling (1901—1994), a giant of twentieth century chemistry, proposed the electroneutrality principle in which electrons distribute themselves in polar covalent molecules so that each atomic charge is nearly neutral. In practice, these charges fall in a range from about +1 to −1. The nonmetals N, O, and F tend to be negatively charged while metals such as Na or Al are positively charged"[19]. We take Crabtree′s definition of the **EN** principle as the advanced version of the originally proposed version. This definition should have been widely accepted since the textbook written by Crabtree is well circulated[19-21]. This principle was said to be very powerful [21], and has been used to explain experimental results[18]. García-Lastra et al. in their research paper stated: "we propose that the color change in the $Al_2O_3 \cdot xCr_2O_3$ series is mainly related to the **EN** principle by Pauling for a transition-metal complex, stating that the total charge of the transition-metal cation in the complex is nearly zero"[22].

Contradictions were also reported and written in textbook, "In apparent contradiction to the electroneutrality principle, there are many complexes in which the metal exists in a low oxidation state and yet is bonded to an element of fairly low electronegativity. Among the most prominent examples are the transition metal

carbonyls, a large class of compounds in which the ligand (CO) is bound to the central metal through carbon. The source of stability in these complexes is the capacity of the carbon monoxide ligand to accept a back donation of electron density from the metal atom"[18]. Although the **EN** principle applies for bonds in compounds formed by elements with low oxidation numbers, whether this principle is also applicable when it comes to compounds containing elements with high formal oxidation numbers, and what are the affecting factors? These questions have not been answered.

Development in computational chemistry makes it possible for us to study charge distribution in molecules. Using natural-population-analysis to obtain the NBO charge, also called the natural atomic charge, to measure the net charge of a specific atom in a molecule or an ion has been widely applied[23-31] and show superiority compared to other methods[59-61]. Density functional theory (DFT) of electronic structure has made an unparalleled impact on the application of quantum mechanics to interesting and challenging problems in chemistry[32]. B3LYP is the most popular and the most widely used of all the DFT functions. It has enjoyed a remarkable performance over a wide range of systems[32]. Batista et al. found that by sufficiently expanding the basis set of the ligands coordinated to the metal ions with polarization functions, the hybrid B3LYP function predicts equilibrium distances and exchange coupling constants of pre-selected spin-electronic states are in excellent agreement with X-ray and magnetic data[33].

Hence, in this work, NBO charges of hexahydrate trivalent ions of $[M(H_2O)_6]^{3+}$ (M=Sc, Ti, V, Cr, Mn, Fe, Co) and $[Co(Ⅲ)L_6]$ (L=F^-, H_2O, NH_3, CN^-) were calculated at B3LYP/6-31++G(d, p) level of DFT. In order to simulate the charges of Al and O atoms in α-Al_2O_3, two Al cluster compounds, $Al_3O(OH)_7(H_2O)_5$ (**Al₃**) and $Al_6O_6(OH)_6(H_2O)_5$ (**Al₆**) were created based on the crystal structure of α-Al_2O_3[34] and their NBO charges were calculated at B3LYP/6-31++G(d, p) level of theory. The results are that except for $[Co(NH_3)_6]^{3+}$, they all violate the **EN** principle by having charges of atoms out of the range of +1 to −1. Contrary to the **EN** principle, we find that the charge of an element is not determined by the element alone, but can be enormously influenced by the type of its immediately adjacent bonding atoms.

1　Calculation method

Here, all calculations for transition metal complexes are carried out with not only polarization functions, but also dispersion functions using Gaussian 09 program[35] at B3LYP/6-31++G(d, p) level of DFT on preselected spin-multiplicity of metal ions based on experimental evidence or arguments. All electrons of metal ions were considered without using effective core potentials (ECPs) and calculated using 6-31++G(d, p) basis set. All calculated structures are true minima, *i.e.*, no imaginary frequency was observed.

Parts of the crystal structure of α-Al_2O_3 were selected and the dangling bonds were terminated with OH^- or H_2O, resulting in neutral $Al_3O(OH)_7(H_2O)_5$ (**Al₃**) and $Al_6O_6(OH)_6(H_2O)_5$ (**Al₆**). The structures of these two compounds were optimized at B3LYP/6-31G(d,p) level of DFT and found to be the true minima. The NBO charges of atoms of the optimized structures were calculated at the same level of theory.

2　Results and discussion

2.1　$[Co(Ⅲ)L_6]^{3-}$ (L=F^-, H_2O, NH_3, CN^-) and the accuracy of the calculation method

Effects of different coordination atoms on the NBO charges of the central metal ion were studied by calculating four $[Co(Ⅲ)L_6]^{3-}$ complexes (only $[CoF_6]^{3-}$ were calculated as a high-spin cation, others as low-spin cations) and the results are given in Fig. 1 and Table 1.

The optimized geometries of $[CoF_6]^{3-}$ and $[Co(CN)_6]^{3-}$ are given in Fig. 2. The calculated Co-C bond length was 0.195 nm for $[Co(CN)_6]^{3-}$, consistent with the experimental value in the solid state (0.191 nm)[36]. It is also known that embedding the complex in a condensed phase lowers the orbital energies and stabilizes the system and the M-L bond lengths would be expected to shorten[37]. Since all calculations treat the complexes as gas phase molecules, the bond distance lengthening is consistent with the above observation.
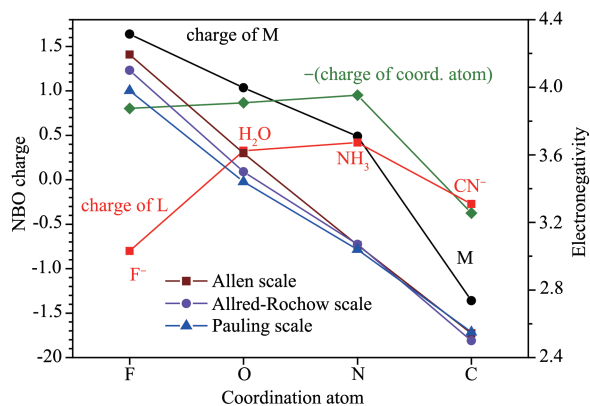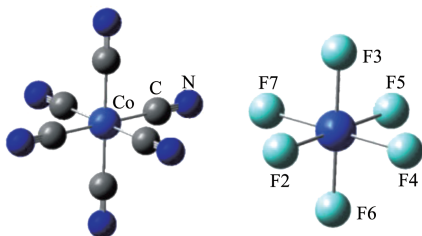
Fig.1　Trend of NBO charge on central cobalt atom, −(charge of coordinated atoms), and each ligand compared with three scale (Pauling′s, Allred-Rochow′s and Allen′s) electronegativity of coordination atoms

Co-C: 0.195 0 nm; Co-F2, F4, F5 or F7: 0.205 5 nm; Co-F3 or F6: 0.191 4 nm

Fig.2　Optimized geometry of $[Co(CN)_6]^{3-}$ and $[CoF_6]^{3-}$

Cotton and Meyers[38] have measured the magnetic moments of $K_3[CoF_6]$ and $Ba_3[CoF_6]_2$ to be 5.25 B.M.~ 5.66 B.M. in a temperature range of 73~299 K, meaning $[CoF_6]^{3-}$ are high spin and have four unpaired electrons. The electronic spectra of various $[CoF_6]^{3-}$ salts suggest that they have static or dynamic Jahn-Teller effect in its structure[38-39]. The calculated Co-F bond lengths were 0.191 4 nm (two bonds along z-axis) and 0.205 5 nm, which are in excellent agreement with the distances (0.194 5 nm (two bonds along z-axis) and 0.206 5 nm) of the optimized geometry at B3LYP meth-

od with def2‐TZVP basis set and Stuttgart RSC 1997 Effective Core Potential by Monajjemi and Khaleghi-an[40]. They also detected the Jahn‐Teller distortion of the high-spin d^6 electronic configuration.

The only available experimental bond distance of Co-F in $[CoF_6]^{3-}$ is obtained as 0.189 nm in CoF_3 structures[41], where Co is six coordinated and thus CoF_3 can be viewed as $[CoF_6]^{3-}$. The structural determination is based on the powder X-ray diffraction pattern determined by Peacock et al. in 1957 assuming it has an octahedral geometry. Their work and a paper by Babel[42] were sometimes wrongly cited as providing structural information for Co-F distance in the $K_3[CoF_6]$ crystal. Thus, the experimental bond distances of Co-F bond distances in $[CoF_6]^{3-}$ still need to be determined, and better determined based on single-crystal XRD diffraction data.

$[Co(H_2O)_6]^{3+}$ is found to have a low‐spin ground state[43-49]. Winkler et al. estimated the energy difference between the low and high spin state is 17.6~19.2 $kJ \cdot mol^{-1}$ [48]. Navon estimated that the lower limit for the difference in the free energies of the low‐spin and high‐spin states of $[Co(H_2O)_6]^{3+}$ is $\Delta G^{\ominus} > 22.6$ $kJ \cdot mol^{-1}$ based on ^{59}Co NMR studies and pointed out that high‐spin state are thermally accessible[49]. $\Delta G^{\ominus}$ were calculated to be (38.1 ± 15.9) $kJ \cdot mol^{-1}$ by Johnson and Nelson based on thermodynamic data[50]. Consistent with the reported results, our calculations also show that high-spin and low spin $[Co(H_2O)_6]^{3+}$ have very similar energy. However, our calculations wrongly predicted that high-spin was the ground state (free energy: −1 840.046 375 Hartree), 14.6 $kJ \cdot mol^{-1}$ more stable than the low-spin ground state (−1 840.040 840 Hartree). Batista et al.[33] reported that the energetics of low-lying spin-states is beyond the capabilities of the DFT/

Table 1　NBO charges of CoL_6 (L=F^-, H_2O, NH_3, CN^-) and other related data

| L | NBO charge | | | Electronegativity of coordination atoms | | | Bond length (M-O) / nm |
	Co	−(coord. atom)*	L	Allen	Pauling	Allred-Rochow	
F^-	1.639	0.802	−0.802	4.19	3.98	4.10	0.206
H_2O	1.034	0.865	0.327	3.61	3.44	3.50	0.192
NH_3	0.489	0.952	0.418	3.07	3.04	3.07	0.203
CN^-	−1.360	−0.375	−0.273	2.54	2.55	2.50	0.195

* Charge divided by −1.

B3LYP level. However, they found that the hybrid B3LYP function predicts equilibrium distances and exchange coupling constants of pre-selected spin-electronic states in excellent agreement with X-ray and magnetic data. The above-mentioned limitation of the DFT/B3LYP level method does not prevent it from being successfully applied in NBO charge calculations[29-31].

It can be seen that from the most positive Co charge in $[CoF_6]^{3-}$ (1.639) to the most negative Co in $[Co(CN)_6]^{3-}$ (−1.360), a large difference (3.0) of charge appears (Fig. 1). Consistently, the diagrams of frontier occupied MOs of $[CoF_6]^{3-}$ (Fig. 3a) shows little or no electron density at Co, but a lot in the diagrams of frontier occupied MOs of $[CoF_6]^{3-}$ (Fig.3b). Only Co (0.489) in $[Co(NH_3)_6]^{3+}$ falls in a range of −1 to +1. Thus, the charge distributions in $[CoF_6]^{3-}$, $[Co(H_2O)_6]^{3+}$ and $[Co(CN)_6]^{3-}$ violate the **EN** principle.

By checking the electron density, ionic or covalent character of coordination bonds can also be studied. Fig. 4 reveal the changes of electron density between $[CoF_6]^{3-}$ and $[Co(CN)_6]^{3-}$ after forming the complexes from the neutral atoms. It could be seen from the electron density diagram (Fig.4a) that when Co and

F form coordination bonds, electron densities decreased among atoms (blue contour lines) while sharp increases were observed in space around the atoms, suggesting ionic natures of Co-F bonds. In contrast, entirely different phenomenon was observed in $[Co(CN)_6]^{3-}$ (Fig.4b). There were significant increases of electron density between C and Co atoms, suggesting covalent nature of Co-C bonds. Thus, from $[CoF_6]^{3-}$ to $[Co(CN)_6]^{3-}$, the character of coordination bonds changes from mainly ionic to mainly covalent.

Another violation of **EN** principle of the above complexes is the preferred charge for the central atoms is enormously influenced by the type of coordination atoms. This result reveals that the chemical environment has significant impact on charges of the central atoms. It appears that the charge of the central metal ion decreases even to negative charge with decreasing electronegativities of coordination atoms, as shown in Table 1 and Fig.1. It is found that when the electronegativity of the coordination atom decreases, electron would not be pulled to the coordination atom but be given to the central atom causing it having a negative charge. NBO analysis revealed that the occupancy of Co-C was 1.90, making it a single bond with bond

MO-44 (b_{1g}) HOMO
Isovalue = 0.015

MO-45 (a_{1g}) LUMO
Isovalue = 0.000 1

MO-42 (a_{2g})
Isovalue = 0.015

MO-43 (a_{1g})
Isovalue = 0.015

MO-40 (e_g)
Isovalue = 0.015

MO-41 (e_g)
Isovalue = 0.015

MO-59 (e_g)
Isovalue = 0.02

MO-60 (e_g)
Isovalue = 0.02

MO-54 (t_{2g}) HOMO
Isovalue = 0.02

MO-55 (a_{1g}) LUMO
Isovalue = 0.000 1

MO-53 (t_{2g})
Isovalue = 0.02

MO-52 (t_{2g})
Isovalue = 0.02
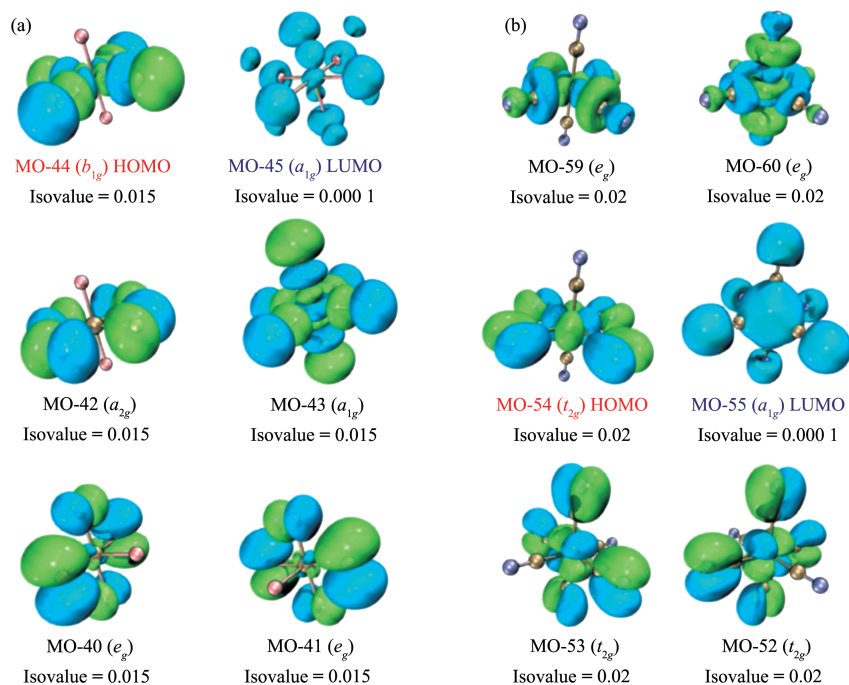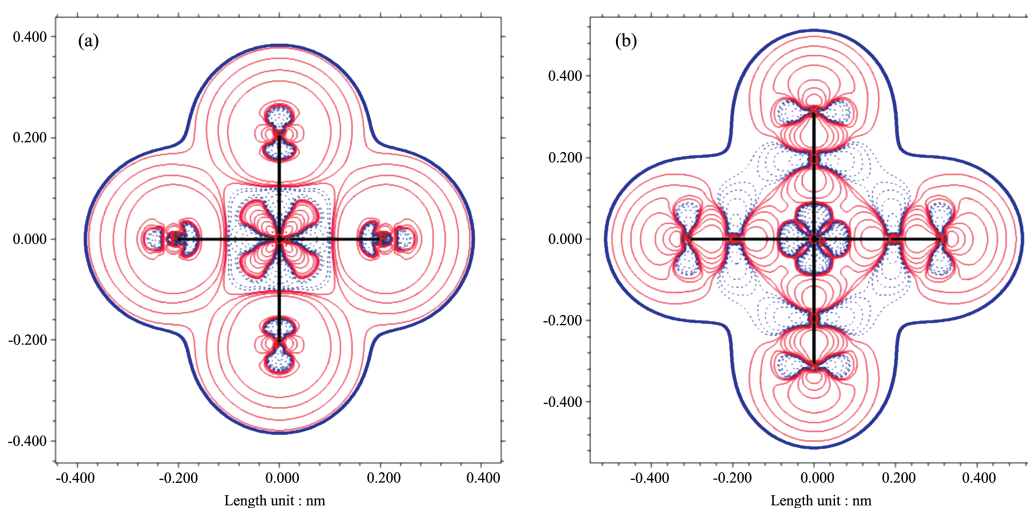
Fig.3　Selected frontier orbital diagrams of $[CoF_6]^{3-}$ (a) and $[Co(CN)_6]^{3-}$ (b) drawn by Multiwfn[58] software

Dotted bule lines and solid red lines indicate the decrease or increase of the electron density after forming coordinating bonds;
Solid blue lines indicate the van der Waals surfaces of complexes

Fig.4　Electron density diagrams of $[CoF_6]^{3-}$ (a) and $[Co(CN)_6]^{3-}$ (b) obtained by subtracting the electron density of the related neutral atoms from the electron density of actual complex using Multiwfn[58] software based on the wavefunction data obtained in the geometry optimization step

order of 0.95. The high positive charge and high negative charge of Co^{3+} in $[CoF_6]^{3-}$ and $[Co(CN)_6]^{3-}$, respectively, were reflected in their frontier oribital digrams and electron density diagrams (Fig. 3 and 4), showing low electron density and high electron density, respectively.

It is also interesting to discover that the negative charge of F, O in H_2O and N in NH_3 did not decreased by following the trend of electronegativity values of these element, but increasing slightly with N in NH_3 bearing the highest charge (Fig. 1), which is probably because H atoms attached to O and N have also transferred some electrons to the coordination atoms, indicating they can have small influence to the central metal ions. The overall charges of the neutral ligands were less than 0.5 (Table 1). The NH_3 ligand bore more positive charge (0.418) than that of H_2O (0.327), consistent with the fact that NH_3 is a better electron donor ligand than H_2O. The CN^- bore much less charges than −1, but only −0.273 (Table 1), indicating large amounts of electrons has been donated to Co^{3+}, making Co become negative charged (−1.360). F^- bore close to −1 charge (−0.802) (Table 1), consistent with the fact that F has the largest electronegativity among all elements except for noble-gas elements. Lone-pair electrons of

F^- also repel the d electrons of Co, which is a destabilizing factor. As a result, the crystal field splitting energy was significantly lower than that of $[Co(CN)_6]^{3+}$ as shown in Fig. 5. The ionic nature of Co-L bonds decreases from F^- to C in CN^- since the NBO charge of Co decreases as shown in Table 1 and their covalent nature of the Co-L bond increases, meaning better overlaps of related atomic orbitals and shorter Co-L bonds (Fig.1).
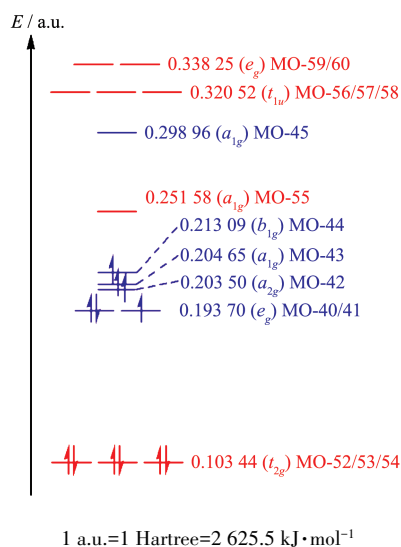

1 a.u.=1 Hartree=2 625.5 kJ·mol^{-1}

Fig.5　Energy levels of selected frontier orbitals (shown in Fig.3) of $[CoF_6]^{3-}$ (in blue) and $[Co(CN)_6]^{3-}$ (in red)

2.2 [M(H₂O)₆]³⁺ (M=Sc~Co)

Since H₂O is a weak field ligand, we calculated all compounds in high-spin states except for Co³⁺ (Table 2). Calculation results show a decline in NBO charge from 1.758 for Sc³⁺ to 1.274 for Cr³⁺, then an increase from Cr³⁺ to Fe³⁺ (1.436) followed a decrease to 1.361 for high spin Co³⁺ (Table 2 and Fig.6~7). Interestingly, there was not even one central metal ion in these hydrates having a charge within −1 to +1. Thus, these examples do not support the **EN** principle. As the electronegativity values of the central atom increases, the corresponding NBO charges generally decreases (Fig.6). The reason is probably that the less electronegativity value the element has, the more positive charge it tends to have. This is not the case for the range from Cr to Co, suggesting other factors might have effect on the charge of the central atom.

Ionic potential values of M³⁺ (Z/r with Z=3) were calculated and given in Fig.7, which have a much better correlation with NBO charges than electronegativity. The trend is when the ionic potential of the central atom increases, its NBO charge decreases. The reason for the above trend is when ionic potential is high, the M³⁺ ion would attract more electrons to itself, reducing its positive charge.

Trends of NBO charges of oxygen atoms and M-O bond lengths (Fig.8) in [M(H₂O)₆]³⁺ correlate well with that of the NBO charges of M. While the charge of M
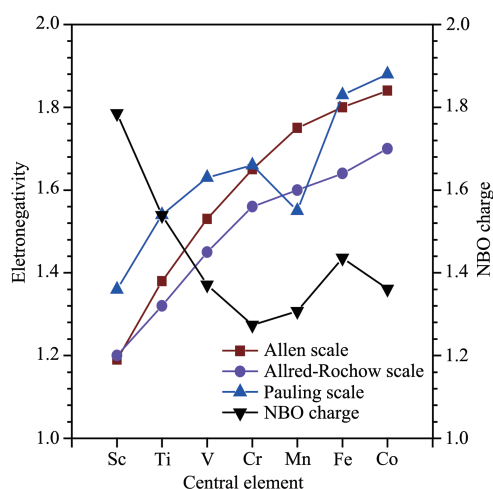
Fig.6 Trend of NBO charges on central transition metal trivalent ions of [M(H₂O)₆]³⁺ (High-spin Co³⁺ data included), compared with three scales (Pauling′s, Allred-Rochow′s and Allen′s) of electronegativity of central transition metal elements
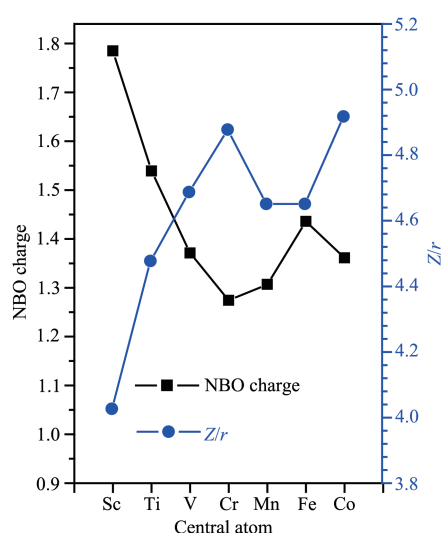
M=Sc~Co, all is in high spin state; Data of r is given in Table 2; Radius of Mn³⁺ is taken as 58 pm[52]

Fig.7 Trend of NBO charge and Z/r of the central atoms of [M(H₂O)₆]³⁺

Table 2 NBO charges of [M(H₂O)₆]³⁺ (M=Sr~Co) and related data

| M | NBO charge | | | Electronegativity of coordination atoms | | | Bond length (M-O) / nm | r / pmᵇ |
	M	−Oᵃ	H	Allen	Pauling	Allred-Rochow		
Sc	1.785	0.973	0.203	1.19	1.36	1.20	0.216	74.5
Ti	1.539	0.935	0.243	1.38	1.54	1.32	0.210	67.0
V	1.371	0.910	0.271	1.53	1.63	1.45	0.205	64.0
Cr	1.274	0.899	0.289	1.65	1.66	1.56	0.201	61.5
Mn	1.307	0.885	0.323	1.75	1.55	1.60	0.197	64.5
Fe	1.436	0.931	0.261	1.80	1.83	1.64	0.205	64.5
CoHᶜ	1.361	0.914	0.274	1.84	1.88	1.70	0.202	61.0
CoLᶜ	1.034	0.865	0.327	1.84	1.88	1.70	0.192	61.0

ᵃ Charge of O divided by −1; ᵇ Radii data of M³⁺ from the reference[51]; ᶜ Co_H or Co_L stands for Co in high-spin or low-spin [Co(H₂O)₆]³⁺.

Fig.8　Trend of NBO charges on O in H_2O, compared with that of high spin central transition metal trivalent ions

decreases, the absolute charge of O decreases. While the absolute NBO charges of M and O decrease, the covalent nature of the M-O bond increases. This means there are more overlaps between M and O′s orbitals and a shorter bond length. Similarly, Co-L bond lengths decrease as the NBO charges of M decreases in the cases of [CoL_6] (Fig.2). When the absolute charge of O decreases, the overall charge of the coordinated H_2O in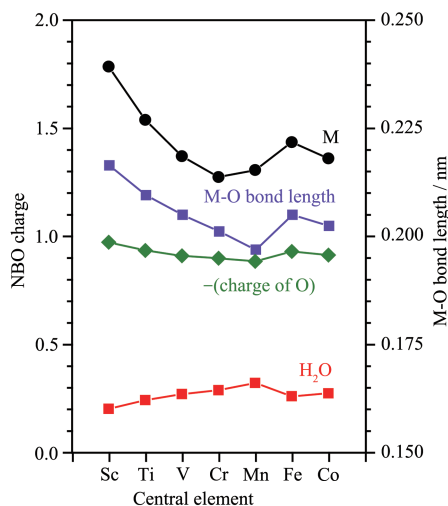creases, implying the charge of H remains constant. The calculated charges of H were 0.587~0.589, 0.589~0.590, 0.590~0.591, 0.594, 0.584~0.604, 0.596, 0.596, 0.593~0.594 for M=Sc, Ti, V, Cr, Mn, Fe, Co (LS), Co(HS), respectively. They are very close with a maximum difference of 0.020.

The charges of O was in a very narrow range (±0.1), which means that the radius of O might be roughly the same from Sc to Co. Thus, the M-O bond length would depend on the radius of M^{3+}. This is supported by the reported experimental radius values of M^{3+} given in Table 1. M-L bond length difference of the adjacent [$M(H_2O)_6$]$^{3+}$ is very similar to the radius difference of the adjacent M^{3+} except for Mn^{3+}, suggesting the radius of Mn^{3+} might not be accurate as also suggested by Fig.7. It should be smaller than 64.5 pm[51]. The radius of Mn^{3+} reported in CRC handbook was 58 pm[52], which gives an improvement of the correlation in Fig.7 and a perfect fit to the calculated Mn-O

bond distance. Since radius of Cr^{3+} (61.5 pm) is 3 pm greater than that of Mn^{3+} (58 pm), the Mn-O bond distance should be 3 pm less than that of Cr-O, which is 0.198 nm, in agreement with the calculated value of 0.197 nm.

We calculated both the low spin ground state and high spin state of [$Co(H_2O)_6$]$^{3+}$ (Table 2). These states are both thermally accessible and low spin state was reported as the ground state (previous section). NBO charge of Co in low-spin [$Co(H_2O)_6$]$^{3+}$ (1.034) was smaller than that (1.361) of high-spin [$Co(H_2O)_6$]$^{3+}$ (Table 2), and the Co-O bond length of low-spin [$Co(H_2O)_6$]$^{3+}$ (0.192 nm) was shorter than that (0.202 nm) of high-spin [$Co(H_2O)_6$]$^{3+}$.

2.3　$Al_3O(OH)_7(H_2O)_5$ (Al_3) and $Al_6O_6(OH)_6(H_2O)_5$ (Al_6)

Parts of the unit cell of α-Al_2O_3 (Fig.S1) were selected and terminated by H_2O or OH^- to create two compounds, Al_3 and Al_6. The optimized geometry of two structures and calculated NBO charges are given in Fig.9 and Table 3. The values were very similar to those obtained by optimizing the structures at B3LYP/6-31G(d) level of DFT and NBO analysis at B3LYP/6-31G(d,p) or B3LYP/6-31++G(d,p) level of DFT (Table S1 and S2). The NBO charges of Al in Al_3 cluster were 6-coordinated and in a narrow range (2.039~2.046). Expanding the cluster to Al_6 did not change greatly the charges of Al, and they are in a range of 2.084~2.127, slightly larger than those of Al_3, except for Al13, which had a charge of 2.039, about 0.10 smaller than the charges of other Al atoms. This Al atom is coordinated with three O^{2-}, and two μ_2-O^{2-} atoms is very close to Al (0.172 9~0.173 0 nm), indicating these two Al-O bonds have significant covalent nature, reducing the charge of the Al atom. In contrast, the Al10-μ_2-O^{2-} distance was 0.182 9 nm. Charges of Al in Al_3 and Al_6 fell in very narrow range (2.0~2.1), depending on which atom (element type and formal charge) it directly connects with, but being not so affected by its coordination number or the type of the atoms two-bonds away. These observations enable us to predict the charge of Al in α-Al_2O_3. It should be around 2.1±0.1. Real space charge density analysis based on the first-principle, self-consistent

H in white, O in red, Al in pink color

Fig.9　Atomic numbers and NBO charges of optimized structures of **Al$_3$** and **Al$_6$**

Table 3　NBO charges of the atoms and ligands of Al$_3$ and Al$_6$

Cluster		**Al$_3$**		**Al$_6$**	
Metal		Atom label, NBO charge, coordination (Ligands)		Atom label, NBO charge, coordination (Ligands)	
Al		6, 2.039, 6c-Al (1 μ_1-H$_2$O, 2 μ_1-OH$^-$, 2 μ_2-OH$^-$, 1 μ_3-O^{2-})[a]		10, 2.084, 5c-Al (1 μ_1-H$_2$O, 1 μ_2-OH$^-$, 1 μ_2-O^{2-}, 2 μ_3-O^{2-})	
		7, 2.041, 6c-Al (2 μ_1-H$_2$O, 1 μ_1-OH$^-$, 2 μ_2-OH$^-$, 1 μ_3-O^{2-})		11, 2.113, 4c-Al (1 μ_1-OH$^-$, 1 μ_2-OH$^-$, 1 μ_2-O^{2-}, 1 μ_3-O^{2-})	
		12, 2.046, 6c-Al (2 μ_1-H$_2$O, 1 μ_1-OH$^-$, 2 μ_2-OH$^-$, 1 μ_3-O^{2-})		12, 2.097, 5c-Al (1 μ_1-OH$^-$, 1 μ_2-OH$^-$, 1 μ_2-O^{2-}, 2 μ_3-O^{2-})	
				13, 2.039, 4c-Al (1 μ_1-H$_2$O, 2 μ_2-O^{2-}, 1 μ_3-O^{2-})	
				14, 2.060, 6c-Al (2 μ_1-H$_2$O, 2 μ_2-OH$^-$, 1 μ_2-O^{2-}, 1 μ_3-O^{2-})	
				15, 2.127, 4c-Al (1 μ_1-H$_2$O, 1 μ_2-OH$^-$, 2 μ_3-O^{2-})	
Ligand		NBO charge of O and (H)[b]	Sum[c]	NBO charge of O and (H)[b]	Sum[c]
H$_2$O	μ_1-	1, −1.197 (17, 0.540; 18, 0.496)	−0.161	7, −1.005 (17, 0.532; 36, 0.540)	0.067
		9, −0.977 (21, 0.531; 29, 0.543)	0.097	22, −1.010 (23, 0.550; 28, 0.515)	0.055
		11, −0.966 (19, 0.530; 30, 0.537)	0.101	26, −1.201 (27, 0.501; 30, 0.540)	−0.160
		14, −0.993 (23, 0.531; 27, 0.541)	0.079	31, −0.996 (32, 0.567; 38, 0.547)	0.118
		15, −1.036 (24, 0.540; 25, 0.522)	0.026	33, −0.988 (34, 0.556; 39, 0.541)	0.109
OH$^-$	μ_1-	3, −1.216 (20, 0.497)	−0.719	18, −1.222 (19, 0.498)	−0.724
		8, −1.256 (22, 0.499)	−0.757	20, −1.044 (21, 0.532)	−0.512
		10, −1.037 (33, 0.530)	−0.507	35, −1.219 (37, 0.507)	−0.712
		16, −1.253 (26, 0.501)	−0.752		
	μ_2-	2, −1.211 (32, 0.523)	−0.688	1, −1.217 (29, 0.541)	−0.676
		4, −1.204 (31, 0.504)	−0.700	9, −1.227 (16, 0.524)	−0.703
		13, −1.205 (28, 0.511)	−0.694	24, −1.197 (25, 0.514)	−0.683
O^{2-}	μ_2-	No μ_2-O^{2-} in this cluster		4, −1.432	
				6, −1.433	
				8, −1.475	
	μ_3-	5, −1.449		2, −1.454	
				3, −1.476	
				5, −1.430	

[a] Numbers of each kind of ligands coordinated with the aluminum atoms were given in parentheses, and 6c-Al stands for hexa-coordinated aluminum atom while 5c- and 4c- stand for penta- and tetra-coordinated; [b] NBO charges of hydrogen atoms connected to the oxygen atoms are given in parentheses; [c] Sum of NBO charges of O and H in each ligand.

orthogonalized linear combination of atomic orbitals (OLCAO) calculations in the local density approximation gave an effective charge formula from $Al_2^{+2.63}O_3^{-1.75}$ to $Al_2^{+2.75}O_3^{-1.83}$ [53]. The experimental values based on common X-ray diffraction data, on the other hand, show that the effective charges on A1 and O were 1.32(5) and −0.88(8), respectively[54]. These numbers are not reliable and tend to underestimate the true values as later discovered by others due to noise, thermal smearing, systematic errors and the X-ray distinction effect[55-56]. Up to date, reliable experimental values for α-Al_2O_3 have not been obtained.

The charges of O in H_2O, OH^- and O^{2-} in **Al₃** were −1.197~ −0.966, −1.256~ −1.037 and −1.449, respectively; for **Al₆**, they were −1.201~ −0.988, −1.227~ −1.044, −1.476~ −1.430, respectively. The actual charges of O were not in huge difference from H_2O (−1.0~ −1.2) to OH^- (−1.0~ −1.2) and O^{2-} (−1.4). The smaller or greater ones are due to hydrogen bonding. For example, the charge of O10 of a OH^- in **Al₃** is −1.037, smaller than those of other OH^-. This is because of O1−H17···O10 hydrogen bonding (O1−H17 0.153 6 nm, O10−H17 0.103 4 nm, ∠O1−H17···O10= 162°), making O10 also resembles O in H_2O, which causes a relative smaller charge.

In summary, the charges of O in OH^-, O^{2-} and Al in **Al₃** and **Al₆** all exceed 1.0, contradicting to the **EN** principle.

3　Conclusions

We find that the **EN** principle is not applicable to complexes or compounds which contains atoms having high formal charges. $[M(H_2O)_6]^{3+}$ (M=Sc, Ti, V, Cr, Mn, Fe, Co), $[Co(Ⅲ)L_6]$ (L=F^-, H_2O, NH_3, CN^-), $Al_3O(OH)_7(H_2O)_5$ and $Al_6O_6(OH)_6(H_2O)_5$, which contain high formal oxidation number atoms, all violates this principle by having atomic charges exceeding +1~ −1. In addition, we find, for compounds having the same charge, that the preferred charge for the central atom is (1) not so influenced by its coordination numbers; (2) not determined by its own electronegativity, but can be enormously influenced by which elements and their formal charges of the directly coordinated atoms and not so

influenced by the atoms two bonds away. Many other examples of compounds having high formal charge atoms violates the **EN** principle. For example, Kuroiwa et al. obtained +1.1 for Pb, +2.4 for Ti and −1.4 for O1 and −1.0 for O_2 in $PbTiO_3$, which were determined by the MEM (maximum entropy method)/Rietveld analysis using synchrotron-radiation powder data[57]. More calculations and experimental works need to be done to give a better statement for the **EN** principle.

We predict that the charge of Al in α-Al_2O_3 is 2.1± 0.1 based on cluster calculations. Reliable experimental charges have not been obtained due to technical problems[55-56], but can be obtained based on high quality X-ray diffraction data obtained by using a synchrotron source and electron diffraction data as done by Zuo et al[55].

In addition, we have the following discoveries. (1) Despite the differences of coordination numbers and ligand type, charges of Al atoms in **Al₃** and **Al₆** fell in a very narrow range (2.0~2.1). The actual charges of O atoms in **Al₃** and **Al₆** are not in huge difference from H_2O (−1.0~−1.2) to OH^- (−1.0~−1.2) to O^{2-} (−1.4). The smaller or greater ones are due to hydrogen bonding. (2) The charges of Co^{3+} in $[CoF_6]^{3-}$ and $[Co(CN)_6]^{3-}$ were found to be 1.639 and −1.360, respectively. (3) When the ionic potential of the central atom increases, its charge would decrease. The M-L bond would have higher covalent nature, and the M-L bond would be shorter as shown in $[M(H_2O)_6]^{3+}$ complexes. (4) The spin state of Co^{3+} strongly affect its charge, which was found to be 1.034 for low-spin state and 1.361 for high spin state. The Co-O bond length of low-spin $[Co(H_2O)_6]^{3+}$ (0.192 pm) is shorter than that (0.202 pm) of high-spin $[Co(H_2O)_6]^{3+}$. (5) Based on the discovered trend, the radius of Mn^{3+} should be 58 pm[52] instead of 64.5 pm[51].

Supporting information is available at http://www.wjhxxb.cn

References:

[1] Wolynes P G. *Ann. Rev. Phys. Chem.*, **1980**,**31**:345-376

[2] Martínez M J, Pappalardo R R, Marcos E S, et al. *J. Phys. Chem. B*, **1998**,**102**:3272-3282

[3] Keyes T, Napoleon R L. *J. Phys. Chem. B*, **2011**,**115**:522-531

[4] Pearson R G. *J. Am. Chem. Soc.*, **1963**,**85**:3533-3539

[5] Pearson R G. *Science*, **1966**,**151**:172-177

[6] Pearson R G. *Chem. Brit.*, **1967**,**3**:103-107

[7] Miranda-Quintana R A, Kim T D, Cárdenas C, et al. *Theor. Chem. Acc.*, **2017**,**136**:135

[8] Cartledge G H. *J. Am. Chem. Soc.*, **1928**,**50**:2855-2863

[9] Cartledge G H. *J. Am. Chem. Soc.*, **1930**,**52**:3076-3083

[10]Feig A L, Panek M, Horrocks W D, et al. *Chem. Biol.*, **1999**,**6**:801-810

[11]Tyler G. *Sci. Total Environ.*, **2004**,**329**:231-239

[12]Fasfous I I, Yapici T, Murimboh J, et al. *Environ. Sci. Technol.*, **2004**,**38**:4979-4986

[13]XU Guang-Xian(徐光宪), ZHAO Xue-Zhuang(赵学庄). *Acta Chim. Sinica*(化学学报), **1956**,**22**:441-446

[14]Sanderson R T. *J. Chem. Educ.*, **1952**,**29**:539-544

[15]Sanderson R T. *J. Chem. Educ.*, **1954**,**31**:2-7

[16]Sanderson R T. *J. Chem. Educ.*, **1954**,**31**:238-245

[17]Pauling L. *J. Chem. Soc.*, **1948**,**23**:1461-1467

[18]Huheey J E, Keiter E A, Kieter R L. *Inorganic Chemistry*: *Principles of Structure and Reactivity*. *4th Ed*. New York: HarperCollins College Publishers, **1993**:393-394

[19]Crabtree R H. *The Organometallic Chemistry of the Transition Metals*. *7th Ed*. Hoboken: John Wiley & Sons, Inc., **2019**:53

[20]Crabtree R H. *The Organometallic Chemistry of the Transition Metals*. *6th Ed*. Hoboken: John Wiley & Sons, Inc., **2014**:27-28

[21]Crabtree R H. *The Organometallic Chemistry of the Transition Metals*. *4th Ed*. Hoboken: John Wiley & Sons, Inc. **2005**: 19-20

[22]García-Lastra J M, Barriuso M T, Aramburu J A, et al. *Phys. Rev. B*, **2009**,**79**:241106

[23]Glendening E D, Badenhoop J K, Reed A E, et al. *NBO* 6.0, *University of Wisconsin*, Madison, WI, USA, **2013**.

[24]Glendening E D, Landis C R, Weinhold F. *J. Comput. Chem.*, **2013**,**34**:1429-1437

[25]Reed A E, Weinstock R B, Weinhold F. *J. Chem. Phys.*, **1985**,**83**:735-746

[26]Weinhold F, Landis C R, Glendening E D. *Int. Rev. Phys. Chem.*, **2016**,**35**:399-440

[27]Wibergand K B, Rablen P R. *J. Comput. Chem.*, **1993**,**14**: 1504-1518

[28]Larin A V, Mortier W J, Vercauteren D P. *J. Comput. Chem.*, **2007**,**28**:1695-1703

[29]Turnbull D, Wetmore S D, Gerken M. *Angew. Chem. Int. Ed.*, **2019**,**58**:13035-13038

[30]Chatterjee K, Dopfer O. *Chem. Sci.*, **2018**,**9**:2301-2318

[31]Yang Y F, Houk K N, Wu Y D. *J. Am. Chem. Soc.*, **2016**,**138**: 6861-6868

[32]Cohen A J, Mori-Sánchez P, Yang W. *Chem. Rev.*, **2012**,**112**: 289-320

[33]Sproviero E M, Gascon J A, McEvoy J P, et al. *J. Inorg. Biochem.*, **2006**,**100**:786-800

[34]Crystallography Open Database (No. 1000017). http://www.crystallography.net/

[35]Frisch M J, Trucks G W, Schlegel H B, et al. *Gaussian* 09, *Revision A*.02, Gaussian, Inc., Wallingford CT, **2016**.

[36]Sophia P, Andrey Z, Julia S, et al. *Cryst. Mater.*, **2018**,**233**:35 -40

[37]Deeth R J, Foulis D L, Williams-Hubbard B J. *Dalton Trans.*, **2003**,**1**:3949-3955

[38]Cotton F A, Meyers M D. *J. Am. Chem. Soc.*, **1960**,**82**:5023-5026

[39]Allen G C, Warren K D. *Struct. Bond.*, **1971**,**9**:49-138

[40]Monajjemi M, Khaleghian M. *J. Clust. Sci.*, **2011**,**22**:673-692

[41]Hepworth M A, Jack K H, Peacock R D, et al. *Acta Crystallogr.*, **1957**,**10**:63-69

[42]Babel D. *Struct. Bond.*, **1967**,**3**:1-87

[43]Friedman H L, Hunt J P, Plane R A, et al. *J. Am. Chem. Soc.*, **1951**,**73**:4028-4030

[44]Johnson D A, Sharpe A G. *J. Chem. Soc. A*, **1966**,**1**:798-801

[45]Nielsen M T, Moltved K A, Kepp K P. *Inorg. Chem.*, **2018**, **57**:7914-7924

[46]Mortensen S R, Kepp K P. *J. Phys. Chem. A*, **2015**,**119**:4041-4050

[47]Johnson D A, Nelson P G. *Inorg. Chem.*, **1999**,**38**:4949-4955

[48]Winkler J R, Rice S F, Gray H B. *Comments Inorg. Chem.*, **1981**,**1**:47-51

[49]Navon G. *J. Phys. Chem.*, **1981**,**85**:3547-3549

[50]Johnson D A, Nelson P G. *J. Chem. Soc. Dalton Trans.*, **1990**,**19**:1-4

[51]Speight J G. *Lange's Handbook of Chemistry*. *16th Ed*. New York: McGRAW-HILL, **2005**:1.153

[52]Lide D R. *CRC Handbook of Chemistry and Physics, Internet Version* 2007. *87th Ed*. Boca Raton: Taylor and Francis, **2007**:12.12. http:/www.hbcpnetbase.com

[53]Ching W Y, Xu Y N. *J. Am. Ceram. Soc.*, **1994,77**:404-411

[54]Lewis J, Schwarzenbach D, Flack H D. *Acta Crystallogr. A*, **1982,38**:733-739

[55]Zuo J M, Kim M, O′Keeffe M, et al. *Nature*, **1999,401**:49-52

[56]Pillet S, Souhassou M, Lecomte C, et al. *Acta Crystallogr. Sect. A*, **2001,A57**:290-303

[57]Kuroiwa Y, Aoyagi S, Sawada A, et al. *Phys. Rev. Lett.*, **2001**, **87**:217601

[58]Lu T, Chen F W. *J. Comput. Chem.*, **2012,33**:580-592

[59]Martin F, Zipse H. *J. Comput. Chem.*, **2005,26**:97-105

[60]Clark A E, Sonnenberg J L, Hay P J, et al. *J. Chem. Phys.*, **2004,121**:2563-2570

[61]LU Tian(卢天), CHEN Fei-Wu(陈飞武). *Acta Phys.-Chim. Sin.*(物理化学学报), **2012,28**(1):1-18